

Onset of Quasideuteron Photodisintegration in ${}^6\text{Li}$ between 25 and 65 MeV

M. W. Wade,^(a) M. K. Brussel, L. J. Koester, Jr., and J. H. Smith

Nuclear Physics Laboratory and Department of Physics, University of Illinois at Urbana-Champaign, Champaign, Illinois 61820

(Received 27 July 1984)

We have measured the energy and angle of coincident np pairs from the reaction ${}^6\text{Li}(\gamma, np)\alpha$ with 67-MeV bremsstrahlung. Quasideuteron correlations were observed as a function of photon energy. The measured quasideuteron transverse momentum distribution was fitted with a $2S$ harmonic-oscillator momentum wave function, yielding a full width at half maximum of 89.4 ± 5.6 MeV/c. Coincident np events from the reaction ${}^6\text{Li}(\gamma, p){}^5\text{He}$ were also observed.

PACS numbers: 25.20.Lj, 27.20.+n

The quasideuteron model of nuclear photodisintegration¹ asserts that an energetic photon interacts with a neutron-proton pair within a complex nucleus, thus driving these nucleons apart with equal and opposite momenta in their c.m. system. Such interactions are said to be with a quasideuteron. Furthermore, the cross section for this process, σ_{qd} , is expected to be proportional to the number of possible pairs, NZ (N is the neutron number; Z is the proton number), the cross section for photodisintegration of a real deuteron, σ_d , and the relative probability that the neutron and proton are interacting strongly (i.e., are close together) in the nucleus compared to the same probability in deuterium. This probability varies inversely with nuclear volume and hence with $A = N + Z$. Thus,

$$\sigma_{qd} = LNZ\sigma_d/A, \quad (1)$$

where Levinger originally calculated the constant L to be 6.4 and later raised this estimate to 8. Experiments at energies above pion threshold verified the expected kinematic correlation of these nucleon pairs in angle^{2,3} and energy.⁴ However, except for low-statistics cloud-chamber experiments⁵ there have been no direct observations of kinematically correlated np pairs to show how the quasideuteron process begins at low energies and grows to its previously observed value as energy increases. This experiment investigates the onset of the quasideuteron process for the nearly ideal case of the reaction ${}^6\text{Li}(\gamma, np){}^4\text{He}$.

A 67-MeV bremsstrahlung beam from the 100%-duty-cycle Illinois Microtron irradiated a thin (24.9 mg/cm²) ${}^6\text{Li}$ target. Protons were identified and their energy measured in a ΔE - E scintillator telescope placed in the horizontal plane at an angle θ_p to the beam (see Fig. 1). The plastic ΔE detector was 5 cm in diameter, 25 cm from the target, and provided the proton timing signal. The E detector was a NaI(Tl) crystal sufficiently wide and thick to stop all protons. Coincident neutrons had their

times of flight measured by a $30 \times 30 \times 7.6$ -cm³ plastic detector 2 m from the target. The neutron detector was at an angle θ_n in the horizontal plane. Energy and angular resolutions as well as the neutron-counter efficiency were measured directly by replacing the ${}^6\text{Li}$ target by $\text{CD}_2\text{-CH}_2$ difference targets.

Figure 2 shows a scatter plot of the neutron energy, T_n , versus the proton energy, T_p , for events obtained at $\theta_n = \theta_p = 84^\circ$. Accidental events (3%) have been subtracted. If the residual ${}^4\text{He}$ remains bound, a measurement of T_n and T_p allows a calculation of the photon energy for each event, and loci for five photon energies defining four experimental photon-energy intervals are plotted on Fig. 2. For calculated photon energies above 43.6 MeV the reaction must leave the ${}^4\text{He}$ intact. We see no marked change in behavior below this energy, and so all our analysis assumes a three-body final state. There is a large group of events with $T_n \approx T_p$ which we interpret as quasideuteron events. For subsequent analysis we define quasideuteron events as those with $\frac{4}{9} < T_n/T_p < \frac{9}{4}$. This region, between the broken lines in Fig. 2, includes almost all of this group of events without including too many extraneous events. A second prominent group near the lowest neutron energies comes from the reac-

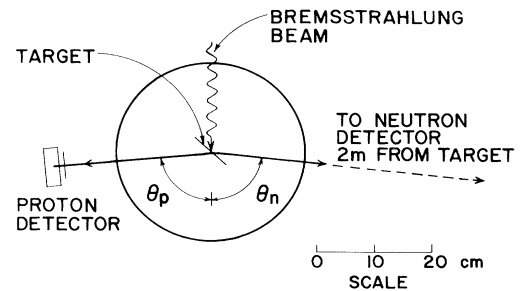


FIG. 1. Experimental geometry. The evacuated target chamber had thin windows for the particles.

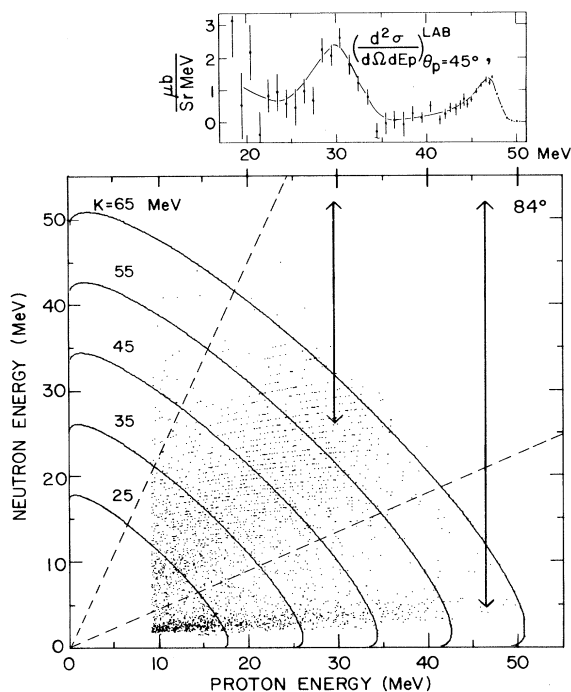


FIG. 2. Scatter plot of correlated np energies from ${}^6\text{Li}(\gamma, np)$ events. Contours represent the constant photon energies indicated. Dotted lines bound quasideuteron events. The proton energy spectrum of Ref. 11 for 60-MeV photons is plotted above for comparison.

tion ${}^6\text{Li}(\gamma, p){}^5\text{He}$ in which the neutron from the breakup of the unstable ground state of ${}^5\text{He}$ is detected.

If the ejected nucleons make no interaction with the residual ${}^4\text{He}$ in the final state, then the sum of their momenta transverse to the beam represents the transverse momentum of the quasideuteron in its initial state. Figure 3 shows graphs of this transverse component of the np -pair momentum for events in each of the four photon-energy bins with both detectors at 84° to the beam. ${}^5\text{He}$ events are not shown. The lowest curve is our result for deuterium and indicates the momentum resolution. The much larger spread in the quasideuteron peaks from ${}^6\text{Li}$ results from the motion of the quasideuteron in the ${}^6\text{Li}$ nucleus. The curves are a numerical calculation from a crude model in which an actual deuteron moves with a $2S$ harmonic-oscillator momentum wave function, as suggested by cluster models.⁶ A Gaussian wave function fits as well, and, until detailed calculations are made involving the magnitude of the cross section, we believe that our data will have little to say about the details of the cluster model. The full width at half maximum

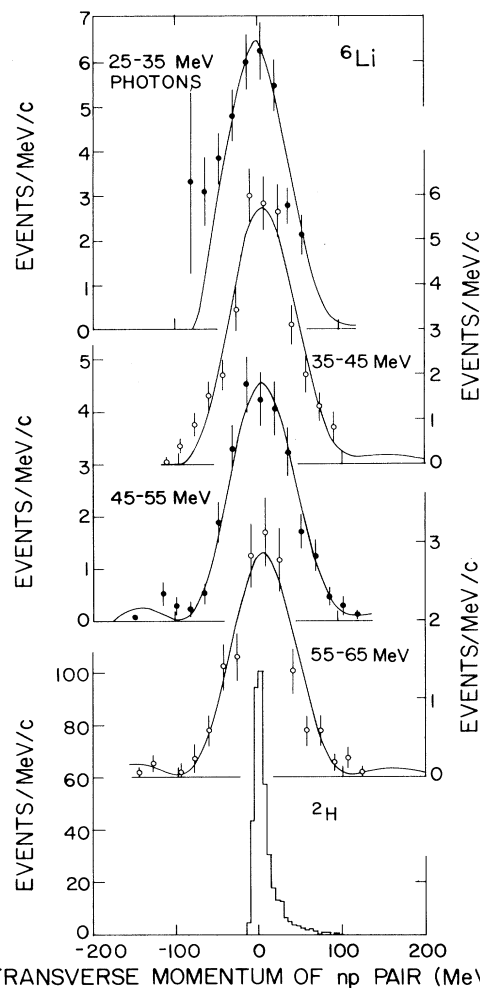


FIG. 3. Distribution of quasideuteron np -pair momentum transverse to the beam for each energy bin. The bottom graph is for ${}^2\text{H}$. Curves are fits by a $2S$ harmonic-oscillator momentum wave function.

is 89.4 ± 5.6 MeV/c in good agreement with ${}^6\text{Li}(\pi^-, nn)$ ⁷ and ${}^6\text{Li}(p, p'd)$ ⁸ experiments but in apparent disagreement with ${}^6\text{Li}(e, e'd)$ and ${}^6\text{Li}(e, e'\alpha)$ experiments.⁹ Within experimental error there seems to be no variation in the momentum spread with photon energy.

Quasideuteron kinematics can be seen in angular correlation measurements as well (see Fig. 4). If both counters are moved forward (or backward), but kept at equal angles to the beam, the counting rate peaks at the opening angle expected for deuterium. The lowest graph in Fig. 4 shows our result from deuterium, and the curve represents the calculated angular resolution. The other four graphs exhibit the spread caused by motion of the quasideuteron in a direction along the photon

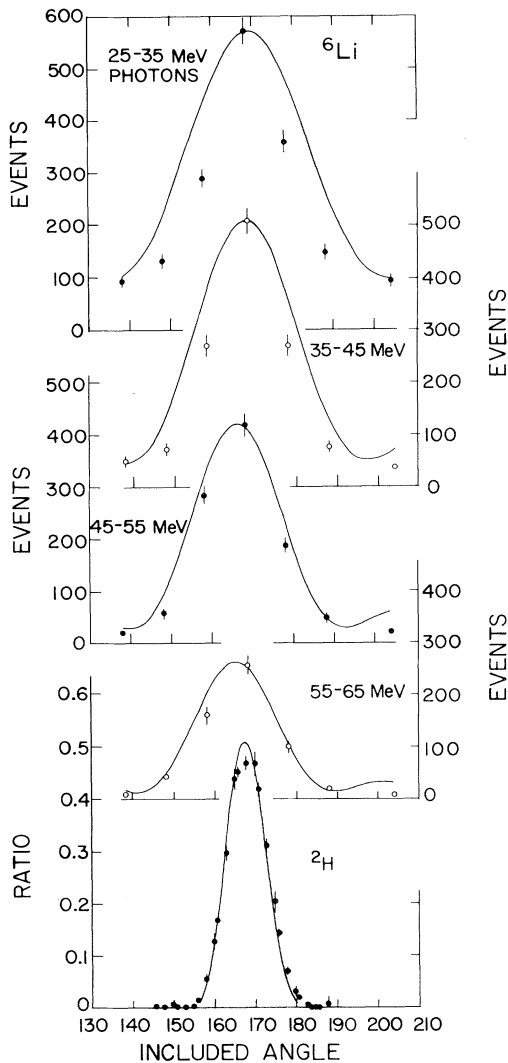


FIG. 4. Quasideuteron coincidence yield vs angle between the detectors for each energy bin. The bottom graph is for ^2H . Curves are discussed in the text.

beam. The photon momentum causes the higher-energy curves to peak at slightly smaller included angles. The solid curves are calculated from the same moving-deuteron model used for the curves in Fig. 3 and with the same momentum parameter. The angular resolution has been folded into the theoretical curves. We have, however, subtracted a fitted constant background unexplained by the simple theory. Although the fit is quite good at the higher energies, it is less satisfactory at the lower ones. Presumably the model is too crude.

The coincidence angular correlation shown in Fig. 4 was integrated over neutron angles to get the quasideuteron cross section $d\sigma_{qd}/d\Omega_p$ at 90° in the

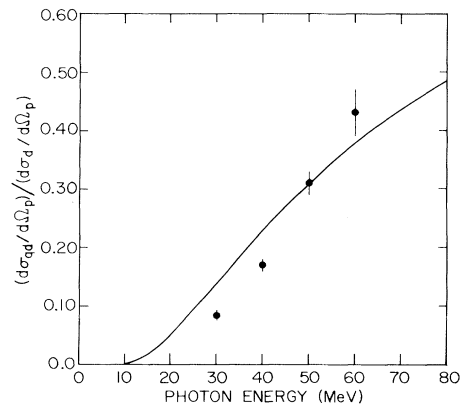


FIG. 5. The quasideuteron/deuteron cross section ratio vs photon energy. The curve is a fit with Levinger's modified quasideuteron model with $D = 60$ MeV.

quasideuteron center-of-mass system as a function of photon energy. The integration was done by the fitting of a Gaussian function plus a constant background to the angular correlation data shown in Fig. 4 under the assumption that the angular dependence out of the horizontal plane is the same as that in that plane. Only the Gaussian part was deemed to represent quasideuterons. Figure 5 shows the results of this integration. To minimize uncertainties in photon monitoring and neutron counter efficiency, $d\sigma_{qd}/d\Omega_p$ is plotted as a ratio to our measured deuteron cross section, $d\sigma_d/d\Omega_p$, also at 90° in the center-of-mass system. That is, an ordinate of 0.5 means that each ^6Li nucleus gives half as many np pairs as would come from a deuteron.

Levinger¹⁰ has speculated that the quasideuteron process should be inhibited by Pauli blocking at these energies and has modified Eq. (1) to read

$$\sigma_{qd} = (LNZ\sigma_d/A)\exp(-D/k), \quad (2)$$

where k is the photon energy, and $D = 60$ MeV is determined by a fit of the total photoabsorption cross section for lead. The curve in Fig. 5 is a fit by this expression and gives a value of $LNZ/A = 1.07 \pm 0.02$. If only the p -shell nucleons are involved, we should take $N = Z = 1$ which gives $L = 6.4 \pm 0.1$. In view of the poor fit by Eq. (2) with $D = 60$ MeV, and the fact that Pauli blocking in lead probably has little relevance for ^6Li , this value should not be taken too seriously.

The proton energy spectrum obtained by Matthews *et al.*¹¹ in a $^6\text{Li}(\gamma, p)$ experiment at 60 MeV is shown above the scatter plot in Fig. 2. The two peaks at 47 and 30 MeV were interpreted as the result of direct knockout from the $1P$ and $1S$ shells, respectively. They report a ratio of 0.39 ± 0.20 for

the areas under those peaks. After integration over angles, assuming isotropic decay of ${}^5\text{He}$, we find a ratio of 0.43 ± 0.17 for p - ${}^5\text{He}$ to quasideuteron events. Although their data are at 45° and our data are for disintegrations near 90° in the center-of-mass system of the np pair, we believe that the similarity suggests that at least a substantial fraction of their 30-MeV peak is from quasideuterons, as emphasized by the arrows in Fig. 2.

We wish to thank Professor A. M. Nathan and the accelerator staff for development and operation of the beam. This work was supported in part by the National Science Foundation under Grant No. NSF PHY 83-11717.

^(a)Present address: AT&T Bell Laboratories, Naperville, Ill.

ville, Ill.

¹J. S. Levinger, Phys. Rev. **84**, 43 (1951).

²M. Q. Barton and J. H. Smith, Phys. Rev. **110**, 1143 (1958).

³P. C. Stein, A. C. Odian, A. Wattenberg, and R. Weinstein, Phys. Rev. **119**, 348 (1960).

⁴I. L. Smith, J. Garvey, J. G. Rutherglen, and G. R. Brooks, Nucl. Phys. **B1**, 483 (1967).

⁵V. N. Fetisov, A. N. Gorbunov, and A. T. Varfolomeev, Nucl. Phys. **71**, 305 (1965).

⁶Y. C. Tang, K. Wildermuth, and L. D. Pearlstein, Phys. Rev. **123**, 548 (1961).

⁷S. Barbarino *et al.*, Phys. Rev. C **21**, 1104 (1980). These authors quote a resolution-corrected full width at half maximum for the experiment reported in H. Davies, H. Muirhead, and J. Woulds, Nucl. Phys. **78**, 663 (1966).

⁸D. Albrecht *et al.*, Nucl. Phys. **A338**, 477 (1980).

⁹J. P. Genin *et al.*, Phys. Lett. **52B**, 46 (1974).

¹⁰J. S. Levinger, Phys. Lett. **82B**, 181 (1979).

¹¹J. L. Matthews, D. J. S. Findlay, S. N. Gardiner, and R. O. Owens, Nucl. Phys. **A267**, 51 (1976).